Bulletin of Earthquake Engineering manuscript No.
(will be inserted by the editor)

Improving FEMA P-58 Non-Structural Component Fragility Functions and Loss Predictions

Gemma Cremen · Jack W. Baker

Received: date / Accepted: date

Abstract Fragility functions are an important tool in earthquake engineering, used to compute the probabilities of different damage states as a function of seismic response. They can be developed for large systems like buildings and bridges, as well as for individual structural and non-structural components, such as those used in the FEMA P-58 Seismic Performance Assessment Procedure. There are currently a number of problems associated with some P-58 non-structural mechanical component fragility functions and related loss predictions, including non-convergence when fitting the fragility functions in some cases and non-monotonic loss predictions. In this study, we recommend improvements to these fragility functions and loss predictions. Firstly, we recommend using the maximum likelihood method to fit the fragility functions to the underlying empirical data. This mitigates the non-convergence problems when fitting and makes predictions that better align with damage observed in past events. To compute predicted losses for anchored mechanical components, it is necessary to additionally consider anchorage damage, which can be predicted using fragility functions based on building code provisions. We recommend refining the current FEMA P-58 method for predicting anchored mechanical component losses, such that component and anchorage damage are calculated directly according to their corresponding fragility functions. The proposed method yields more intuitive loss predictions that vary monotonically with anchorage capacity. It also leads to better predictions of losses relative to damage observed in previous events. If implemented, the recommendations made in this paper would enhance the FEMA P-58 Seismic Performance Assessment Procedure.

G. Cremen
439 Panama Mall Room 214, Stanford University, Stanford, CA 94305.
Tel.: +1-650-2857054
E-mail: gcremen@stanford.edu

J.W. Baker
473 Via Ortega Room 283, Stanford University, Stanford, CA 94305.

Keywords Non-Structural Components · Fragility Functions · Loss Predictions · FEMA P-58

1 Introduction

Fragility functions are used in earthquake engineering to compute the probabilities of different damage states as a function of seismic response. Originally created to characterize the seismic risk of nuclear power plants (Kennedy and Ravindra, 1984), they can be developed for large systems such as buildings and bridges (e.g. Akkar et al., 2005; Huo and Zhang, 2012), as well as individual structural and non-structural components (e.g. Choe et al., 2008; Lopez Garcia and Soong, 2003). They are typically calculated using earthquake reconaissance data (e.g. Colombi et al., 2008; Rota et al., 2008), experimental observations (e.g. Pagni and Lowes, 2006; Gardoni et al., 2002), structural analysis results (e.g. Rota et al., 2010; Nielson, 2005), and/or expert opinion (Mosleh and Apostolakis, 1986). Numerous statistical techniques exist in the literature for fitting fragility functions to the underlying data (Lallemant et al., 2015), but they do not all yield equivalent functions.

The FEMA P-58 Seismic Performance Assessment Procedure (FEMA, 2012a), a performance-based earthquake engineering methodology for individual buildings based primarily on US construction data, provides a database of structural and non-structural component fragility functions for building damage calculations. In this study, we examine some FEMA P-58 non-structural mechanical component fragility functions that were derived from post-earthquake reconnaissance data and experimental observations. These fragility functions currently have a number of associated problems, including non-convergence issues in some cases. We recommend a change to the current fragility function fitting technique, and demonstrate the benefits of the proposed procedure.

To compute predicted losses for anchored mechanical components, it is necessary to additionally consider anchorage damage. This can be predicted using fragility functions derived from building code provisions, or case-specific failure modes if sufficient anchorage detail is available. The current FEMA P-58 procedure for predicting anchored mechanical component losses involves pre-selecting a damage mode that is dependent on differences in the component and anchorage fragility functions, and consequently the resulting damage predictions do not correspond to the individual fragility functions. This procedure can lead to unexpected results, including non-smooth variation of repair costs as a function of median anchorage capacity. We recommend refining this procedure such that the damage predictions are directly calculated according to both the component and the anchorage fragility functions, and show the advantages of this approach.

2 Fitting Fragility Functions from Empirical Data

A fragility function is used to determine the probability that the damage state (DS) will reach or exceed a given damage state of interest (ds_k), conditioned on the value of an appropriate engineering demand parameter (EDP), such as peak floor acceleration or story drift ratio, or intensity measure (e.g. spectral acceleration). It is typically modeled as a lognormal cumulative distribution function (e.g. Singhal and Kiremidjian, 1996; Rossetto and Elnashai, 2005; Porter et al., 2007; Sarabandi et al., 2004; Porter et al., 2001; Badillo-Almaraz et al., 2007). That is,

$$P(DS \geq ds_k | EDP = edp_i) = \Phi\left(\frac{\ln\left(edp_i/\theta\right)}{\beta}\right) \tag{1}$$

where $P(DS \geq ds_k | EDP = edp_i)$ is the probability of being in or exceeding ds_k when $EDP = edp_i$, $\Phi(.)$ is the standard normal cumulative distribution function (CDF), θ is the median of the fragility function, i.e. the value of EDP such that $P(DS \geq ds_k | EDP = \theta) = 50\%$, and β is the standard deviation of $\ln EDP | ds_k$. It can be seen from equation 1 that a fragility function is completely defined by the θ and β parameters.

We focus on FEMA P-58 fragility functions for non-structural mechanical components with known installation conditions that were fit using empirical data from both post-earthquake reconnaissance efforts and experimental observations in Porter (2011). These are Method B ('Bounding EDP') type data, as they contain observations of both damage and no damage, and there is information on the maximum $EDPs$ to which all specimens were subjected (Porter et al., 2007; Bradley, 2010). EDP in this case is the estimated peak floor acceleration at the appropriate level in a building (PFA). Note that there is only one damage state (denoted ds_1) associated with a given component. Each component is either unanchored and not vibration isolated (installation category 1), vibration isolated but not snubbed or restrained (installation category 2), or vibration isolated/ hard anchored with seismic restraints (installation category 3).

The functions are currently fit to the empirical data using a least-squares curve fitting method. We recommend that the functions are instead fit using maximum likelihood estimation. The proposed fitting procedure mitigates the problem of non-convergence that can occur for the current fitting procedure with data that contain low proportions of damage. It also offers a number of other advantages.

2.1 Proposed Fitting Procedure

We recommend using the maximum likelihood method to fit these fragility functions. This method has previously been proposed for fitting fragility functions with similar data (e.g. Lallemant et al., 2015; Shinozuka et al., 2000). Assume that in a given dataset, there are n components, m of which were

damaged. The likelihood that an arbitrary component is damaged at a level of demand that caused damage (edp_i) is the normal distribution probability density function (PDF) evaluated at the fragility function defined by equation 1, i.e.,

$$\text{Likelihood} = \phi\left(\frac{\ln\left(edp_i/\theta\right)}{\beta}\right) \tag{2}$$

where $\phi(.)$ is the normal distribution PDF. For the $n-m$ components that were not damaged, we know that the maximum EDP to which they were subjected (edp_{max}) is less than the level that would cause damage (edp_i). The likelihood that an arbitrary component is not damaged at edp_{max} is the probability that edp_i exceeds edp_{max}, i.e.,

$$\text{Likelihood} = 1 - \Phi\left(\frac{\ln\left(edp_{max}/\theta\right)}{\beta}\right) \tag{3}$$

where $\Phi(.)$ is the standard normal CDF. Assuming independence of edp_i values, the likelihood of the given dataset being observed is the product of the likelihoods for each component, i.e.,

$$\text{Likelihood} = \left[\prod_{i=1}^{m} \phi\left(\frac{\ln\left(edp_i/\theta\right)}{\beta}\right)\right]\left[1 - \Phi\left(\frac{\ln\left(edp_{max}/\theta\right)}{\beta}\right)\right]^{n-m} \tag{4}$$

The fragility function parameters are the values of θ and β that maximize this likelihood. We maximize the logarithmic likelihood instead, since it is easier and produces equivalent results, i.e.,

$$\{\hat{\theta}, \hat{\beta}\} = \underset{\theta,\beta}{\text{argmax}} \sum_{i=1}^{m}\left[\ln \phi\left(\frac{\ln(edp_i/\theta)}{\beta}\right)\right] + [n-m]\ln\left[1 - \Phi\left(\frac{\ln(edp_{max}/\theta)}{\beta}\right)\right] \tag{5}$$

where θ is positive. For consistency with the current P-58 fragility function fitting procedure, we constrain the value of β between 0.2 and 0.6.

2.2 Current P-58 Fitting Procedure

The P-58 fragility functions are currently fit using a least-squares curve-fitting method, detailed in Porter (2011). This involves minimizing the sum of the squared differences between the fraction of components damaged and the corresponding probability of damage calculated according to the lognormal CDF, for each unique value of PFA observed i.e.,

$$\{\hat{\theta}, \hat{\beta}\} = \text{argmin}\left[\frac{1}{M}\sum_{i=1}^{N} M_i\left(y_i - \Phi\left(\frac{\ln\left(x_i/\theta\right)}{\beta}\right)\right)^2\right] \tag{6}$$

where M is the number of components in the dataset, M_i is the number of components in bin i, y_i is the fraction of damaged components in bin i, N is the number of bins of constant excitation, and x_i is the PFA associated with bin i. θ is positive and β has a value between 0.2 and 0.6.

2.3 Comparison of Fitting Results

The two procedures can result in very similar fragility functions (Figure 1(a)), or significantly different functions (Figure 1(b)), depending on the underlying data. We examined all components with Method B type data in Porter (2011). A summary of all mechanical component fragility parameters calculated using both procedures is found in Table 1. The proposed procedure reduces the value of θ for 15 out of the 21 components examined, and increases the value of θ for all other components. The reduction in θ is more than 40% for 6 out of the 21 components examined, while the maximum increase in θ is 19%. The proposed procedure either maintains (for 11 components), increases (for 9 components) or decreases (for 1 component) the value of β obtained in the current P-58 procedure. Increases in β are as large as 200% for 3 components, while the only decrease in β is 23%.

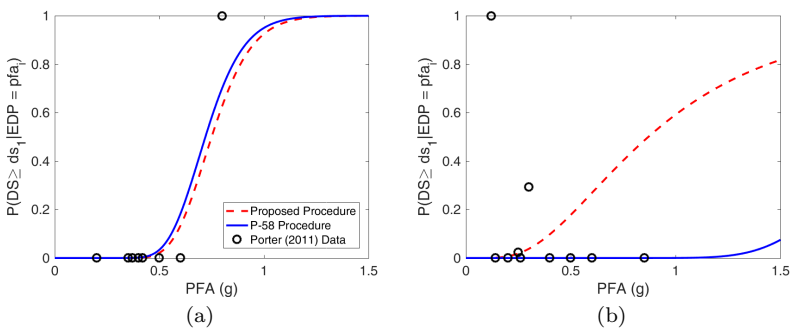

Fig. 1 Comparing the fragility functions obtained using both procedures for (a) chiller (installation category 3) and (b) diesel generator (installation category 3). The fragility functions are almost identical in (a), where the proposed procedure yields respective θ and β values of 0.75 and 0.20, and the current P-58 procedure yields respective θ and β values of 0.72 and 0.20. The fragility parameters differ significantly in (b), where the proposed procedure yields respective θ and β values of 0.87 and 0.60, and the current P-58 procedure yields respective θ and β values of 2.00 and 0.20.

2.4 Advantages of the Proposed Fitting Procedure

2.4.1 Mitigates Non-Convergence Problems

The current P-58 fitting procedure does not always converge to a solution for data sets with low proportions of damage (Porter, 2011). An alternative procedure has to be used in such cases instead, which was created for fitting data with no damage and therefore makes a number of simplifying assumptions (Porter et al., 2007). It computes θ by creating a subjective damage probability

Table 1 Comparison of mechanical component fragility parameters obtained using the proposed and current P-58 fragility function fitting procedures. The data used to fit the fragility functions can be found in Porter (2011). * indicates a parameter value for which the current P-58 fitting procedure did not converge, and a simplified fitting strategy was employed. There were no convergence issues using the proposed procedure for any of the components.

Component	Installation Category	θ		β	
		Proposed	P-58	Proposed	P-58
Battery Charger	3	1.55	2.70	0.60	0.60
Battery Rack	1	0.81	1.11	0.60	0.60
Battery Rack	3	2.56	2.32	0.60	0.20
Chiller	2	0.51	0.43	0.60	0.60
Chiller	3	0.75	0.72	0.20	0.20
Compressor	2	0.48	0.47	0.20	0.20
Compressor	3	1.13	1.84	0.60	0.60
Control Panel	3	1.29	2.61	0.60	0.20
Cooling Tower	2	0.92	0.97	0.46	0.60
Diesel Generator	3	0.87	2.00	0.60	0.20
Distribution Panel	3	3.40	3.05	0.60	0.40
HVAC Fan	2	0.95	1.01	0.60	0.60
HVAC Fan	3	2.12	4.82	0.60	0.60
Low Voltage Switchgear	3	1.37	2.40	0.60	0.40
Motor Control Center	1	0.87	0.73	0.60	0.45
Air Handling Unit	3	1.34	1.54	0.60	0.60
Transformer	2	0.89	1.01	0.60	0.60
Transformer	3	2.49	3.05	0.60	0.60
Motor Control Center	3	1.24	2.50*	0.60	0.40*
Control Panel	1	0.64	0.69*	0.60	0.40*
Diesel Generator	1	0.84	0.90*	0.60	0.40*

for specimens subjected to the higher end of the tested range of EDP, dependent on the level of distress in the specimen as determined by the analyst, and uses an assumed value of $\beta = 0.4$. The proposed procedure always converges to a solution for the data examined, however. It was successfully used to fit data for the three cases in Porter (2011) that experienced non-convergence for the current P-58 procedure. The parameters obtained using both procedures are summarized at the bottom of Table 1 for these three cases. It can be seen that the proposed procedure produces a significantly lower θ value for the motor control center, and similar θ values for the other two components. Note that the proposed procedure increases the value of β by 50% in all three cases.

2.4.2 Damage Predictions Better Align With Observed Damage

To study consistency of damage probabilities with observed damage data, we examine given buildings that were damaged in the 1994 M_w 6.7 Northridge earthquake, using post-earthquake inspection data from the Strong Instrumentation Program (SMIP) Information System (Naeim, 1997; Naeim and Lobo, 1998). We use component damage data reported on ATC-38 post-earthquake damage assessment forms (Rojahn, 2000), which are included in the SMIP In-

formation System. Component damage is classified into 'None', 'Insignificant', 'Moderate', and 'Heavy' categories on this form. We focus on the roof level of each building, and choose components from Table 1 that were likely installed at the roof in each building (chiller, air handling unit, motor control center, transformer, and distribution panel). Damage probabilities for each component are computed using equation 1, with EDP equal to the maximum acceleration recorded at the roof amplified by a factor of 1.2 (pfa_{roof}), in line with the FEMA P-58 methodology for components not sensitive to directionality (FEMA, 2012a).

Damage probabilities for the chiller are compared with damage recorded in the 'Damage to Boilers, Chillers, Tanks, etc.' category of the ATC-38 form. Damage probabilities for the air handling unit are compared with damage recorded in the 'HVAC Damage (Fans, Ducts)' category of the form. Damage probabilities for the motor control center, the transformer, and the distribution panel are compared with damage recorded under the 'Electrical Equipment Damage Including Backup Generators' category of the form. We assume that all of the components were seismically restrained (installation category 3), based on photographic evidence (Naeim, 1997, personal communication).

Figure 2 compares observed damage with the damage probabilities calculated using both procedures for each component. The mean damage probability for a given observed damage level is the mean of all damage probabilities calculated for that observed damage level. It can be seen from Figure 2 that there is not a consistent increase in mean damage probability with observed damage level for the current P-58 fragility function fitting procedure, as the mean damage probabilities for 'Moderate' and 'High' observed damage levels are effectively identical. However, there is a consistent increase in mean damage probability with observed component damage level for the proposed fragility function fitting procedure. The fragility functions fit using the proposed procedure produce damage probabilities that better align with the damage observed for these buildings than those fit using the current P-58 procedure. The Figure 2 data can be found in Section 5.1 of the Appendix.

2.4.3 Fragility Parameters Are More Effectively Estimated

An important property of the data used to fit these fragility functions is the heteroskedasticity of variance for different observed probabilities of damage (Kaufman, 2013). This means that an error in fitting of 0.1 when the observed probability of damage is 0 is significantly larger than a fitting error of 0.1 when the observed probability of damage is 0.4. The presence of heteroskedasticity violates the conditions necessary for the current P-58 procedure of least-squares fitting (Agresti, 2013), but it is accounted for in the proposed procedure.

The proposed procedure produces more efficient fragility estimates than the current P-58 procedure. We can compare the efficiency of fragility functions fit with both procedures, using the method outlined in Baker (2015). We use the 65 acceleration values observed for the battery rack (installation

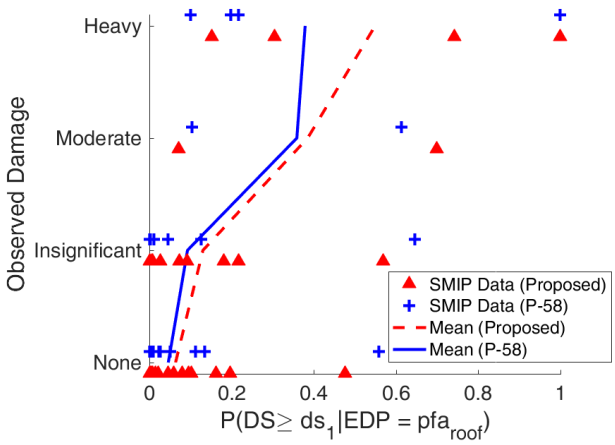

Fig. 2 Damage probabilities for components at the roof level in the Northridge buildings calculated using fragility functions fit with the proposed procedure and the current P-58 procedure, plotted against component damage observed. The mean damage probability for a given observed damage level is the mean of all damage probabilities calculated for that observed damage level.

category 1) in Porter (2011), which range from $0.30g$ to $0.79g$. We assume the true fragility function has $\theta = 0.70$ and $\beta = 0.30$. We use 500 Monte Carlo simulations to generate damage or no damage at each of the acceleration values of interest (using probabilities from the assumed fragility function), and fit fragility functions on each set of generated data using both procedures. We measure the efficiency by calculating the standard deviations of repeated parameter estimates; the higher the efficiency, the lower the standard deviations (Baker, 2015). The proposed procedure reduces the standard deviation of θ estimates by 13% (Figure 3), and the standard deviation of β estimates by 18% (Figure 4).

The proposed procedure reduces epistemic uncertainty due to having finite data. We can measure this uncertainty for fragility functions fit with both procedures, using bootstrapping (Bradley, 2010). We examine the 58 data points for the HVAC fan (installation category 2) from Porter (2011), with acceleration values ranging from $0.35g$ to $0.88g$. We fit fragility functions for both procedures using 500 bootstrap samples of the data. The closer the fitted fragility function is to the mean bootstrapped result, the lower the epistemic uncertainty due to finite sample uncertainty. The mean result from bootstrapping at a given value of PFA is the mean probability of damage calculated at that value across all bootstrap samples. Figure 5 shows the absolute difference in damage probability between the fitted function and the mean bootstrapped result for both procedures across a range of values of PFA. It can be seen that the fragility function fit using the proposed procedure more closely follows the associated mean bootstrap result than that fit using the current P-58 procedure. Note that for the bootstrapping method to work, it is important

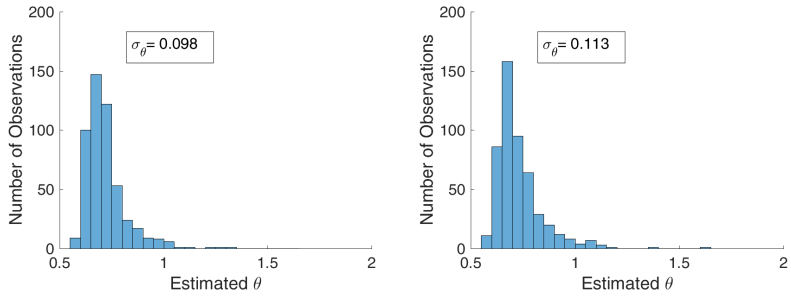

(a) (b)

Fig. 3 Histogram of estimated θ values for (a) the proposed fragility function fitting procedure and (b) the current P-58 fragility function fitting procedure. The standard deviation of the estimates is noted in both plots.

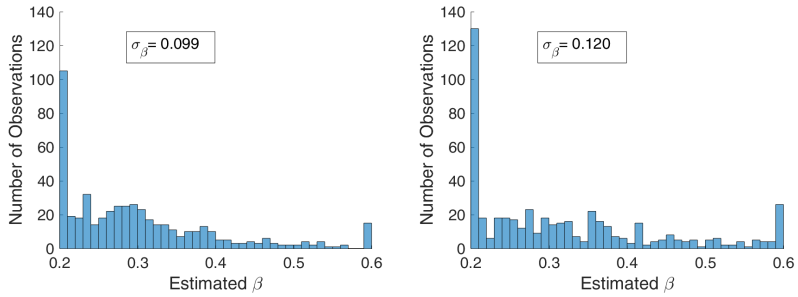

(a) (b)

Fig. 4 Histogram of estimated β values for (a) the proposed fragility function fitting procedure and (b) the current P-58 fragility function fitting procedure. The standard deviation of the estimates is noted in both plots.

to choose a data set with a high proportion of damage, so that there are some damage observations in each bootstrapped sample, and the damage observations should be reasonably well distributed across the range of PFA.

3 Predicting Losses for Anchored Components

To predict losses for anchored mechanical components (installation categories 2 and 3), it is necessary to consider anchorage damage in addition to the component (henceforth referred to as 'equipment') damage described in Section 2. Anchorage damage can be predicted using fragility functions based on building code provisions in effect at the time of installation, or based on case-specific failure modes if sufficient anchorage detail is available. When predicting losses for anchored components, we recommend that probabilities of damage for the anchorage and the equipment are directly calculated according to their respec-

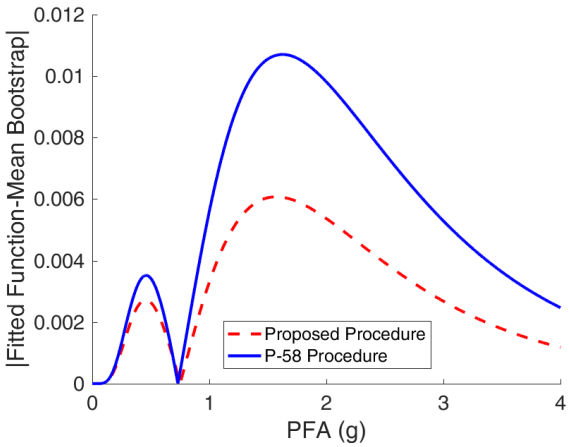

Fig. 5 Comparing the fitted fragility function with the mean result from bootstrapping. The fragility function fit using the proposed procedure more closely follows the mean bootstrap result than that fit using the current P-58 procedure, indicating that the proposed fragility function has lower epistemic uncertainty due to finite sample uncertainty.

tive fragility functions. The total loss prediction is then the sum of the losses to the anchorage and the equipment.

The proposed approach differs from the current P-58 procedure, in which predicting the losses involves pre-selecting a damage mode depending on the difference in the anchorage and equipment median capacities. The damage mode determines the occurrence of both anchorage and equipment failure, such that the resulting damage predictions do not directly correspond to the individual anchorage and equipment fragility functions. The current P-58 procedure yields some unexpected results, including non-monotonic variation of repair costs with median anchorage capacity. The proposed procedure always leads to smooth variation of repair costs, and offers other benefits.

3.1 Current P-58 Loss Prediction Procedure

The current P-58 procedure for predicting anchored mechanical component losses assumes that damage occurs according to a pre-selected damage mode, which is determined based on the difference in the median equipment capacity and the median anchorage capacity. The loss (e.g. repair cost) for the equipment and anchorage is then exclusively the loss associated with this damage mode. There are three possible damage modes (FEMA, 2012b):

1. **Anchorage failure (a)**. If the median anchorage capacity (θ_a) is less than 30% of the median equipment capacity (θ_e), this mode assumes that the anchorage fails well before the equipment. There are two mutually exclusive damage states in this damage mode, i.e. anchorage failure only (ao), and both anchorage and equipment failure (ae). The anchorage fragility function describes the probability of occurrence of this damage mode. The

expected repair cost prediction for $EDP = edp_i$ (RC_a) is calculated as follows:

$$RC_a = P(DS \geq a|EDP = edp_i) \times [x_1 \times RC_{ao} + (1 - x_1) \times RC_{ae}] \quad (7)$$

where $P(DS \geq a|EDP = edp_i)$ is the probability of occurrence of a according to the anchorage fragility function, x_1 is the conditional probability of occurrence of ao given a, RC_{ao} is the repair cost for ao, and RC_{ae} is the repair cost for ae.

2. **Equipment failure (e)**. If θ_e is less than 30% of θ_a, this mode assumes that the equipment fails well before the anchorage. There are N mutually exclusive damage states in this damage mode (e_j) that describe different types of equipment damage, with the highest representing equipment failure. The empirical equipment fragility function describes the probability of occurrence of this damage mode. The expected repair cost prediction for $EDP = edp_i$ (RC_e) is calculated as follows:

$$RC_e = P(DS \geq e|EDP = edp_i) \times \sum_{j}^{N} y_j \times RC_{e_j} \quad (8)$$

where $P(DS \geq e|EDP = edp_i)$ is the probability of occurrence of e according to the equipment fragility function, y_j is the conditional probability of occurrence of e_j given e, and RC_{e_j} is the repair cost associated with e_j.

3. **Combined failure (c)**. For all other values of θ_a and θ_e, this mode assumes simultaneous failure of anchorage and equipment. There are three mutually exclusive damage states associated with this damage mode, i.e. anchorage failure only (ao), anchorage and equipment failure (ae), and equipment failure (e). e involves the N mutually exclusive damage states of the equipment failure damage mode (e_j). The anchorage fragility function describes the probability of occurrence of this damage mode. The expected repair cost prediction for $EDP = edp_i$ (RC_c) is calculated as follows:

$$RC_c = P(DS \geq c|EDP = edp_i) \times [x_2 \times RC_{ao} + x_3 \times RC_{ae} + x_4 \times \sum_{j}^{N} z_j \times RC_{e_j}] \quad (9)$$

where $P(DS \geq c|EDP = edp_i)$ is the probability of occurrence of c according to the anchorage fragility function, x_2, x_3, and x_4 are the conditional probabilities of occurrence of ao, ae, and e respectively given the occurrence of c, and z_j is the conditional probability of occurrence of e_j given e. RC_{ao}, RC_{ae}, and RC_{e_j} are as defined in the other two damage modes.

3.2 Proposed Loss Prediction Procedure

In the proposed procedure, the probabilities of anchorage and equipment damage are calculated directly according to the the anchorage and equipment fragility functions. This means that the anchorage and equipment failure damage modes of the current P-58 procedure are still used, but they can occur simultaneously instead of one of them being pre-selected. The total mean loss

prediction is the sum of mean losses predicted for the two damage modes, minus loss from equipment damage double counted in both modes. The expected repair cost prediction for $EDP = edp_i$ (RC) is calculated as follows:

$$RC = P(DS \geq a|EDP = edp_i) \times [x_1 \times RC_{ao} + (1 - x_1) \times RC_{ae}] + P(DS \geq e|EDP = edp_i) \times \sum_{j}^{N} y_j \times [1 - (1 - x_1) \times P(DS \geq a|EDP = edp_i)] \times RC_{e_j} \tag{10}$$

where all variables are as defined in equations 7 - 9.

3.3 Comparison of Loss Results

Here, we compare the two procedures for chiller and distribution panel components (both installation category 3) by examining expected repair cost predictions across ranges of both EDP (i.e. PFA) and median anchorage capacity (θ_a). We assume that the β value for the anchorage fragility function (β_a) is 0.5 in all cases, which is consistent with FEMA P-58 directions for code-based fragility functions. Other relevant parameters for the two components are obtained from the FEMA P-58 methodology, and are summarized in Table 2. Note that there is only one equipment damage state (e_1) for both components.

Table 2 Fragility and repair cost data for components to be compared under both procedures.

Component	θ_e		β_e		x_1, x_2, x_3, x_4	RC_{ao}	RC_{e_1}	RC_{ae}
	Proposed	P-58	Proposed	P-58				
Chiller	0.75	0.72	0.20	0.20	0.70,0.35,0.15,0.50	1100	50,820	51,920
Distribution Panel	3.40	3.05	0.60	0.40	0.70,0.35,0.15,0.50	1440	61,680	63,120

3.3.1 Chiller

Loss predictions for the chiller component are shown in Figure 6. It can be seen in Figures 6(a) and 6(b) that the proposed procedure results in higher expected repair cost predictions for most values of PFA and θ_a examined. This is because the median capacity of the equipment (which dominates the repair cost) is small relative to much of the range of median anchorage capacities examined, which dictate the probability of equipment damage for the current P-58 procedure in both damage modes that feature for the values of PFA and θ_a examined (i.e. anchorage failure and combined failure). Section 5.2 in the Appendix contains sample calculations of expected repair cost using both procedures, for $PFA = 1g$ and $\theta_a = 1g$.

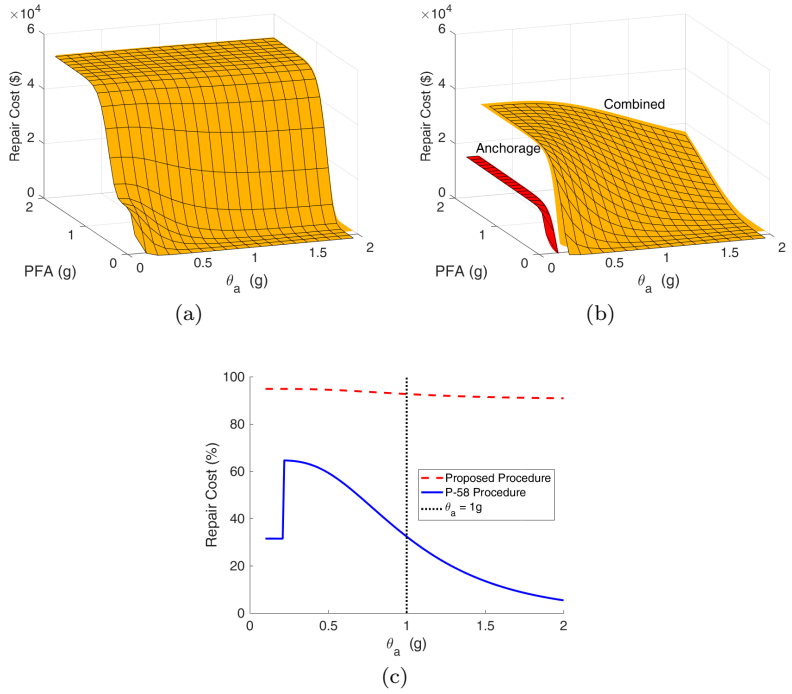

Fig. 6 Expected repair cost predictions for the chiller component over a range of θ_a and PFA, calculated using (a) the proposed procedure and (b) the current P-58 procedure. The two predictions are compared for $PFA = 1g$ in (c) using expected repair cost as a percentage of the maximum repair cost. Note that in (b), the red color denotes expected repair costs controlled by the anchorage failure damage mode (calculated using equation 7), and the orange color denotes expected repair costs controlled by the combined failure damage mode (calculated using equation 9).

3.3.2 Distribution Panel

Loss predictions for the distribution panel component are shown in Figure 7. It can be seen in Figures 7(a) and 7(b) that the proposed procedure results in lower expected repair costs for most values of PFA and θ_a examined. This is because the median capacity of the equipment (which dominates the repair cost) is large relative to much of the range of median anchorage capacities examined, which dictate the probability of equipment damage for the current P-58 procedure in both damage modes that feature for the values of PFA and θ_a examined (i.e. anchorage failure and combined failure). Section 5.2 in the Appendix contains sample calculations of expected repair cost using both procedures, for $PFA = 1g$ and $\theta_a = 1g$.

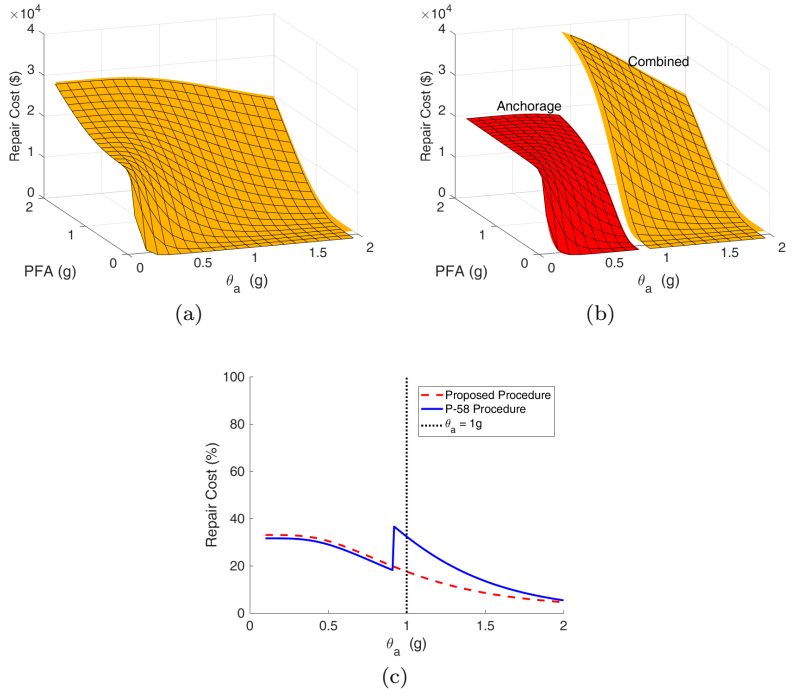

Fig. 7 Expected repair cost predictions for the distribution panel component over a range of θ_a and PFA, calculated using (a) the proposed procedure and (b) the current P-58 procedure. The two predictions are compared for $PFA = 1g$ in (c) using expected repair cost as a percentage of the maximum repair cost. Note that in (b), the red color denotes expected repair costs controlled by the anchorage failure damage mode (calculated using equation 7), and the orange color denotes expected repair costs controlled by the combined failure damage mode (calculated using equation 9).

3.4 Advantages of the Proposed Procedure

3.4.1 Loss Predictions Vary Smoothly and Intuitively

It is clear from Figures 6(c) and 7(c) that there are discontinuities in expected repair costs predicted using the current P-58 procedure across different values of θ_a for a given value of PFA ($PFA = 1g$ in these cases). The discontinuities occur at the values of θ_a where the damage mode changes. There is smooth variation of expected repair costs across different values of θ_a given PFA for the proposed procedure.

As the median anchorage capacity increases, the current P-58 procedure can result in higher expected repair costs if the damage mode changes. This can be observed for $PFA = 1g$ in Figures 6(c) and 7(c). This is not intuitive, as we anticipate the expected repair cost to decrease if the anchorage becomes less vulnerable. The proposed procedure produces repair costs that intuitively decrease monotonically with increasing median anchorage capacity.

3.4.2 Loss Predictions Better Align with Observed Damage

To demonstrate this, we use the same building and component data from Section 2.4.2. We calculate anchorage fragility functions according to ASCE/SEI 7-10 provisions (ASCE, 2010), which require the use of short period spectral acceleration (S_{DS}) values to calculate median anchorage capacity. We obtain S_{DS} values for each building using the USGS seismic design map tool for ASCE/SEI 7-10, assuming soil category D for each site. Calculations of anchorage capacity and component repair cost data (obtained from the FEMA P-58 methodology) are summarized in Section 5.3 of the Appendix. Expected repair cost predictions are carried out exactly according to the calculations in Section 3.3.

Figure 8 compares observed damage with expected repair costs (as a percentage of the associated maximum repair cost) calculated using both procedures for each component. The mean repair cost percentage for a given observed damage level is the mean of all expected repair cost percentages associated with the given observed damage level. It can be seen from Figure 8 that the proposed loss prediction procedure produces repair cost percentage estimates that are more consistent with the observed level of damage; there is a clear increase in mean repair cost percentage prediction as the observed damage level increases, while the current P-58 loss prediction procedure produces effectively identical mean repair cost percentage predictions for components that were insignificantly or moderately damaged.

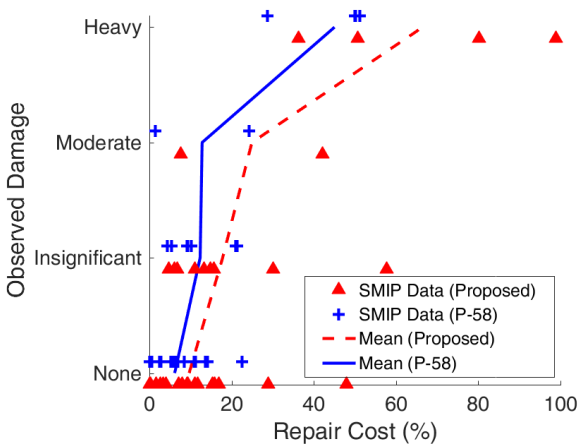

Fig. 8 Expected repair cost percentages for components at the roof level in the Northridge buildings, calculated using the proposed procedure and the current P-58 procedure, plotted against component damage observed. The mean repair cost percentage for a given observed damage level is the mean of all expected repair cost percentages calculated for that observed damage level.

3.4.3 Procedure is Consistent with Code Prescriptions

According to design standards underlying United States codes (e.g ASCE, 2010, 2016), mechanical component equipment capacities are only calculated using code procedures for equipment pieces with importance factors (I_p) greater than 1, which are those typically required to function for life-safety purposes after an earthquake. In these cases, the capacities of the equipment and its associated anchorage are calculated using the same equation in the code and are therefore identical to each other. In all other cases (i.e. $I_p = 1$), which include all of the components examined in this study, only the capacity of the anchorage is calculated according to code provisions and the equipment capacity can be obtained from an empirical fragility function. This is exactly adhered to in the proposed procedure. However, the current P-58 procedure follows code provisions for $I_p > 1$ in the combined failure damage mode, where it assumes that equipment capacities are identical to anchorage capacities.

4 Conclusions

Fragility functions are an important tool in earthquake engineering for computing the probabilities of different damage states as a function of seismic response. In this study, we have made several recommendations for improving non-structural mechanical component fragility functions and associated loss predictions in the FEMA P-58 Seismic Performance Assessment Procedure. Revised procedures were proposed, and several benefits of the proposal were illustrated.

Firstly, we have recommended re-fitting P-58 fragility functions for non-structural mechanical components derived from empirical data, using maximum likelihood estimation. The proposed fitting procedure mitigates non-convergence issues that arise in certain cases for the current P-58 fitting procedure, makes predictions that better align with observed damage in past events, and more efficiently estimates fragility parameters, among other benefits.

To compute loss predictions for anchored mechanical components, anchorage damage also needs to be considered. This is typically derived using a fragility function based on building code provisions or case-specific anchorage failure details. The current FEMA P-58 procedure for computing anchored mechanical component loss predictions involves pre-selecting a damage mode that depends on differences between the component and anchorage fragility functions, and consequently the resulting damage predictions do not correspond to the individual fragility functions. This procedure can lead to unexpected results, including non-smooth variation of repair costs as a function of median anchorage capacity, and increased repair costs as the anchorage becomes less vulnerable. We have recommended refining this procedure, such that damage is predicted directly in line with the component and anchorage fragility functions. The proposed procedure leads to repair cost predictions that vary smoothly as a function of median anchorage capacity and decrease monotoni-

cally as anchorage becomes less vulnerable. In addition, repair cost predictions are more consistent with damage observed in previous events.

If implemented, the recommendations made in this paper would enhance the FEMA P-58 Performance Assessment Procedure, an important tool in seismic design and risk analysis practice.

Acknowledgements We thank an anonymous reviewer for comments that improved the quality of this manuscript. We appreciate helpful feedback received from Dustin Cook, Curt Haselton, Katie Fitzgerald Wade, and Brendon Bradley. We thank Farzad Naeim for providing a copy of the SMIP Information System, and for feedback on typical equipment installation conditions.

References

Agresti A (2013) Categorical data analysis. John Wiley & Sons

Akkar S, Sucuoğlu H, Yakut A (2005) Displacement-based fragility functions for low-and mid-rise ordinary concrete buildings. Earthquake Spectra 21(4):901–927

ASCE (2010) Minimum design loads for buildings and other structures, ASCE/SEI 7-10. American Society of Civil Engineers

ASCE (2016) Minimum design loads for buildings and other structures, ASCE/SEI 7-16. American Society of Civil Engineers

Badillo-Almaraz H, Whittaker AS, Reinhorn AM (2007) Seismic fragility of suspended ceiling systems. Earthquake Spectra 23(1):21–40

Baker JW (2015) Efficient analytical fragility function fitting using dynamic structural analysis. Earthquake Spectra 31(1):579–599

Bradley BA (2010) Epistemic uncertainties in component fragility functions. Earthquake Spectra 26(1):41–62

Choe DE, Gardoni P, Rosowsky D, Haukaas T (2008) Probabilistic capacity models and seismic fragility estimates for rc columns subject to corrosion. Reliability Engineering & System Safety 93(3):383–393

Colombi M, Borzi B, Crowley H, Onida M, Meroni F, Pinho R (2008) Deriving vulnerability curves using Italian earthquake damage data. Bulletin of Earthquake Engineering 6(3):485–504

FEMA (2012a) FEMA P-58-1: Seismic Performance Assessment of Buildings. Volume 1–Methodology. Federal Emergency Management Agency Washington, DC

FEMA (2012b) FEMA P-58-2: Seismic Performance Assessment of Buildings. Volume 2–Implementation Guide. Federal Emergency Management Agency Washington, DC

Gardoni P, Der Kiureghian A, Mosalam KM (2002) Probabilistic capacity models and fragility estimates for reinforced concrete columns based on experimental observations. Journal of Engineering Mechanics 128(10):1024–1038

Huo Y, Zhang J (2012) Effects of pounding and skewness on seismic responses of typical multispan highway bridges using the fragility function method. Journal of Bridge Engineering 18(6):499–515

Kaufman RL (2013) Heteroskedasticity in regression: Detection and correction, vol 172. Sage Publications

Kennedy R, Ravindra M (1984) Seismic fragilities for nuclear power plant risk studies. Nuclear Engineering and Design 79(1):47–68

Lallemant D, Kiremidjian A, Burton H (2015) Statistical procedures for developing earthquake damage fragility curves. Earthquake Engineering & Structural Dynamics 44(9):1373–1389

Lopez Garcia D, Soong T (2003) Sliding fragility of block-type non-structural components. part 1: Unrestrained components. Earthquake engineering & structural dynamics 32(1):111–129

Mosleh A, Apostolakis G (1986) The assessment of probability distributions from expert opinions with an application to seismic fragility curves. Risk analysis 6(4):447–461

Naeim F (1997) Seismic performance of extensively instrumented buildings an interactive information system. CSMIP Report

Naeim F, Lobo R (1998) Performance of non-structural components during the January 17, 1994 Northridge Earthquake–case studies of six instrumented multistory buildings. In: Proceedings of the Seminar on Seismic Design, Retrofit, and Performance of Nonstructural Components, ATC-29-1, San Francisco, CA, Citeseer, pp 107–119

Nielson BG (2005) Analytical fragility curves for highway bridges in moderate seismic zones. PhD thesis, Georgia Institute of Technology

Pagni CA, Lowes LN (2006) Fragility functions for older reinforced concrete beam-column joints. Earthquake Spectra 22(1):215–238

Porter K (2011) Fragility of Mechanical, Electrical. and Plumbing Equipment Considering Installation Conditions. BD-3.9.10. Federal Emergency Management Agency Washington, DC

Porter K, Kennedy R, Bachman R (2007) Creating fragility functions for performance-based earthquake engineering. Earthquake Spectra 23(2):471–489

Porter KA, Kiremidjian AS, LeGrue JS (2001) Assembly-based vulnerability of buildings and its use in performance evaluation. Earthquake spectra 17(2):291–312

Rojahn C (2000) Database on the performance of structures near strong-motion recordings: 1994 Northridge, California, earthquake, vol 38. The Applied Technology Council

Rossetto T, Elnashai A (2005) A new analytical procedure for the derivation of displacement-based vulnerability curves for populations of RC structures. Engineering structures 27(3):397–409

Rota M, Penna A, Strobbia C, Magenes G (2008) Direct derivation of fragility curves from Italian post-earthquake survey data. In: Proceedings of the 14th World Conference on Earthquake Engineering, Beijing, China, October, pp 12–17

Rota M, Penna A, Magenes G (2010) A methodology for deriving analytical fragility curves for masonry buildings based on stochastic nonlinear analyses. Engineering Structures 32(5):1312–1323

Sarabandi P, Pachakis D, King S, Kiremidjian A (2004) Empirical fragility functions from recent earthquakes. In: Proceedings of the 13th World Conference on Earthquake Engineering, Vancouver, BC, Canada. Paper

Shinozuka M, Feng MQ, Lee J, Naganuma T (2000) Statistical analysis of fragility curves. Journal of engineering mechanics 126(12):1224–1231

Singhal A, Kiremidjian AS (1996) Method for probabilistic evaluation of seismic structural damage. Journal of Structural Engineering 122(12):1459–1467

5 Appendix

5.1 Comparing Mechanical Component Damage Predictions with Observed Damage

Table 3 Comparing mechanical component damage probabilities (calculated using the proposed and current P-58 fragility function fitting procedures) with component damage observed in the SMIP Information System for Northridge buildings, as described in Section 2.4.2. Note that Observed Damage and $P(DS \geq ds_1|EDP = pfa_{roof})$ are reported in the following order: chiller, air handling unit, motor control center, transformer, distribution panel. For Observed Damage, N = 'None', I='Insignificant', M = 'Moderate', and H = 'Heavy'. Note that the values of pfa_{roof} include the 1.2 amplification factor required by FEMA P-58 for components not sensitive to directionality.

pfa_{roof} (g)	$P(DS \geq ds_1\|EDP = pfa_{roof})$		Observed Damage
	Proposed	P-58	
0.74	(0.48,0.16,0.20,0.02,0.01)	(0.56,0.11,0.00,0.01,0.00)	(N,N,N,N,N)
1.83	(1.00,0.70,0.75,0.30,0.15)	(1.00,0.61,0.22,0.20,0.10)	(H,M,H,H,H)
0.58	(0.10,0.08,0.10,0.01,0.00)	(0.14,0.05,0.00,0.00,0.00)	(N,N,N,N,N)
0.56	(0.07,0.07,0.09,0.01,0.00)	(0.10,0.05,0.00,0.00,0.00)	(M,I,I,I,I)
0.78	(0.57,0.18,0.22,0.03,0.01)	(0.65,0.13,0.00,0.01,0.00)	(I,I,I,I,I)
0.48	(0.01,0.04,0.06,0.00,0.00)	(0.02,0.03,0.00,0.00,0.00)	(N,N,N,N,N)
0.23	(0.00,0.00,0.00,0.00,0.00)	(0.00,0.00,0.00,0.00,0.00)	(N,N,N,N,N)

5.2 Sample Calculations of Anchored Component Repair Cost Predictions

Let $EDP = 1g$ and $\theta_a = 1g$ for both components. All other variable values are summarized in Table 2 of Section 3.3.

5.2.1 Chiller

Proposed Procedure
First, calculate the probability of anchorage damage with equation 1, using

the anchorage fragility parameters:

$$P(DS \geq a|EDP = 1) = \Phi\left(\frac{\log(1/1)}{0.5}\right) = 0.50 \tag{11}$$

Then, calculate the probability of equipment damage with equation 1, using the equipment fragility parameters:

$$P(DS \geq e|EDP = 1) = \Phi\left(\frac{\log(1/0.75)}{0.2}\right) = 0.92 \tag{12}$$

Finally, compute the expected repair cost using equation 10:

$$RC = 0.50\times[0.70\times1100+(1-0.70)\times51,920]+0.92\times[1-(1-0.70)\times0.50]\times50,820 = \underline{\mathbf{\$48,121}} \tag{13}$$

$$RC\% = \frac{RC}{RC_{ae}} \times 100 = \frac{48,121}{51,920} \times 100 = \underline{\mathbf{93\ \%}} \tag{14}$$

Current P-58 Procedure
Since $0.3 \times \theta_e \leq \theta_a$ and $0.3 \times \theta_a \leq \theta_e$, select combined failure damage mode. First, calculate the probability of occurrence of the damage mode with equation 1, using the anchorage fragility parameters:

$$P(DS \geq c|EDP = 1) = \Phi\left(\frac{\log(1/1)}{0.5}\right) = 0.50 \tag{15}$$

Then, compute the expected repair cost using equation 9:

$$RC = 0.50 \times [0.35 \times 1100 + 0.15 \times 51,920 + 0.50 \times 50,820] = \underline{\mathbf{\$16,792}} \tag{16}$$

$$RC\% = \frac{RC}{RC_{ae}} \times 100 = \frac{16,792}{51,920} \times 100 = \underline{\mathbf{32\ \%}} \tag{17}$$

Even though the probability of equipment failure is significant in this case, the expected repair cost predicted using the current P-58 procedure is low since it is restricted by the lower vulnerability of the anchorage.

5.2.2 Distribution Panel

Proposed Procedure
First, calculate the probability of anchorage damage with equation 1, using the anchorage fragility parameters:

$$P(DS \geq a|EDP = 1) = \Phi\left(\frac{\log(1/1)}{0.5}\right) = 0.50 \tag{18}$$

Then, calculate the probability of equipment damage with equation 1, using the equipment fragility parameters:

$$P(DS \geq e|EDP = 1) = \Phi\left(\frac{\log(1/3.40)}{0.6}\right) = 0.02 \tag{19}$$

Finally, compute the expected repair cost using equation 10:

$$RC = 0.50\times[0.70\times1440+(1-0.70)\times63,120]+0.02\times[1-(1-0.70)\times0.50]\times61,680 = \underline{\mathbf{\$11,057}} \tag{20}$$

$$RC\% = \frac{RC}{RC_{ae}} \times 100 = \frac{11,057}{63,120} \times 100 = \underline{\mathbf{18\ \%}} \tag{21}$$

Current P-58 Procedure
Since $0.3 \times \theta_e \leq \theta_a$ and $0.3 \times \theta_a \leq \theta_e$, select combined failure damage mode. First, calculate the probability of occurrence of the damage mode with equation 1, using the anchorage fragility parameters:

$$P(DS \geq c|EDP = 1) = \Phi\left(\frac{\log(1/1)}{0.5}\right) = 0.50 \tag{22}$$

Then, compute the expected repair cost using equation 9:

$$RC = RC_c = 0.50 \times [0.35 \times 1440 + 0.15 \times 63,120 + 0.50 \times 61,680] = \underline{\mathbf{\$20{,}406}} \tag{23}$$

$$RC\% = \frac{RC}{RC_{ae}} \times 100 = \frac{20,406}{63,120} \times 100 = \underline{\mathbf{32\ \%}} \tag{24}$$

Even though the probability of equipment failure is extremely low in this case, the repair cost predicted using the current P-58 procedure is relatively large as it is inflated by the higher vulnerability of the anchorage.

5.3 Comparing Anchored Mechanical Component Repair Cost Predictions with Observed Damage

5.3.1 Calculating Anchorage Capacity

To calculate anchorage capacity, it is first necessary to obtain the anchorage system design resistance (ϕR_n), which is calculated according to ASCE/SEI 7-10 equations 13.3-1 - 13.3-3 as follows:

$$\phi R_n = \frac{F_p}{W_p} = \frac{0.4 \times a_p \times S_{DS} \times (1 + 2\frac{z}{h})}{\frac{R_p}{I_p}} \tag{25}$$

$$\phi R_n \leq 1.6 \times S_{DS} \times I_p \tag{26}$$

$$\phi R_n \geq 0.3 \times S_{DS} \times I_p \tag{27}$$

where a_p is a component amplification factor (assumed to be 1 for all components examined since we are calculating capacity), S_{DS} is the short period spectral acceleration value (see Table 5 in Section 5.3.3 for building-specific values), h is the height of the building relative to the ground, z is the height of the component in the building relative to the ground (equal to h in this case, since we are considering roof-level components), I_p is the component importance factor (equal to 1 for all components examined in this study) and R_p is a component response modification factor (equal to 2.5 or 6 for components examined in this study, depending on the component of interest). We assume that the anchorage has the brittle failure modes typical for concrete anchorage (FEMA, 2012b), so the relevant equation to calculate median capacity is equation 3-2 in FEMA (2012a):

$$\theta = C_q \times e^{(2.81\beta)} \times \phi R_n \tag{28}$$

where θ is the median anchorage capacity, C_q is an adjustment coefficient for construction quality, and β is the β parameter for the anchorage fragility function. C_q and β are both set equal to 0.5, in accordance with FEMA (2012b).

5.3.2 Component Repair Cost Data

Table 4 Repair cost data for the components examined in Northridge buildings.

Component	x_1	y_1	y_2	x_2	x_3	$x_4 \times z_1$	$x_4 \times z_2$	RC_A	RC_{e_1}	RC_{e_2}	RC_{ae}
Chiller	0.70	1.00	$\sim$	0.35	0.15	0.50	$\sim$	1100	50,820	$\sim$	51,920
Air Handling Unit	0.70	0.67	0.33	0.35	0.15	0.35	0.15	2640	2200	204,600	207,240
Motor Control Center	0.70	1.00	$\sim$	0.35	0.15	0.50	$\sim$	550	4565	$\sim$	5115
Transformer	0.70	1.00	$\sim$	0.35	0.15	0.50	$\sim$	1100	8333	$\sim$	9433
Distribution Panel	0.70	1.00	$\sim$	0.35	0.15	0.50	$\sim$	1440	61,680	$\sim$	63,120

5.3.3 Comparing Predictions and Observations

Table 5 Comparing expected component repair cost percentage predictions (calculated using the proposed and current P-58 procedures) with component damage observed in the SMIP Information System for Northridge buildings, as outlined in Section 3.4.2. Note that Observed Damage and Expected Repair Cost % are reported in the following order: chiller, air handling unit, motor control center, transformer, distribution panel. For Observed Damage, N = 'None', I='Insignificant', M = 'Moderate', and H = 'Heavy'. Note that the values of pfa_{roof} include the 1.2 amplification factor required by FEMA P-58 for components not sensitive to directionality.

pfa_{roof} (g)	S_{DS}	Expected Repair Cost %		Observed Damage
		Proposed	P-58	
0.74	1.46	(48,16,29,15,11)	(6,11,23,14,11)	(N,N,N,N,N)
1.83	2.00	(99,42,80,51,36)	(29,24,50,50,51)	(H,M,H,H,H)
0.58	1.39	(11,9,17,9,7)	(3,7,14,8,7)	(N,N,N,N,N)
0.56	1.56	(8,7,13,6,5)	(1,4,9,9,9)	(M,I,I,I,I)
0.78	1.59	(58,16,30,15,11)	(5,10,21,21,21)	(I,I,I,I,I)
0.48	1.57	(2,4,8,3,3)	(1,3,5,5,5)	(N,N,N,N,N)
0.23	1.48	(0,0,0,0,0)	(0,0,0,0,0)	(N,N,N,N,N)